

SLAC-PUB-7373

UTEXAS-HEP-96-21

DOE-ER-40757090

December 1996

Probing Contact Interactions at High Energy Lepton Colliders *

Kingman Cheung¹, Stephen Godfrey², and JoAnne Hewett³

¹University of Texas, Austin TX 78712

²Ottawa Carleton Institute for Physics, Carleton University, Ottawa, Canada

³Stanford Linear Accelerator Center, Stanford, CA 94309

Abstract

Fermion compositeness and other new physics can be signalled by the presence of a strong four-fermion contact interaction. Here we present a study of $\ell\ell qq$ and $\ell\ell\ell'\ell'$ contact interactions using the reactions: $\ell^+\ell^- \rightarrow \ell'^+\ell'^-, b\bar{b}, c\bar{c}$ at future e^+e^- linear colliders with $\sqrt{s} = 0.5 - 5$ TeV and $\mu^+\mu^-$ colliders with $\sqrt{s} = 0.5, 4$ TeV. We find that very large compositeness scales can be probed at these machines and that the use of polarized beams can unravel their underlying helicity structure.

To appear in the *Proceedings of the 1996 DPF/DPB Summer Study on New Directions for High Energy Physics - Snowmass96*, Snowmass, CO, 25 June - 12 July, 1996.

1 Introduction

There is a strong historical basis for the consideration of composite models which is presently mirrored in the proliferation of fundamental particles. In attempts to explain the repetition of generations or the large number of arbitrary parameters within the Standard Model (SM), several levels of substructure have been considered[1], including composite fermions, Higgs bosons, and even weak bosons. Here we focus on the possibility that leptons and quarks are bound states of more fundamental constituents, often referred to as preons in the literature. The preon binding force should be confining at a mass scale Λ which also characterizes the radius of the bound states. Experimentally, Λ is constrained to be at least in the TeV range. Theoretically, numerous efforts have been made to construct realistic models for composite fermions, but no consistent or compelling theory which accounts for $m_{\ell,q} \ll \Lambda$ presently exists. At energies above Λ the composite nature of fermions would be revealed by the break-up of the bound states in hard scattering processes. At lower energies, deviations from the SM may be observed via form factors or residual effective interactions induced by the binding force. These composite remnants are usually parameterized by the introduction of contact terms in the low-energy lagrangian. More generally, four fermion contact interactions represent a useful parameterization of many types of new physics originating at a high energy scale, such as the exchange of new gauge bosons, leptoquarks, or excited particles, or the existence of anomalous couplings.

These contact interactions are described by non-renormalizable operators in the effective low-energy lagrangian. The lowest order four-fermion contact terms are dimension-6 and hence have dimensionful coupling constants proportional to g_{eff}^2/Λ^2 . The fermion currents are restricted to be helicity conserving, flavor diagonal, and $SU(3) \otimes SU(2) \otimes U(1)$ invariant. These terms can be written most generally as[2, 3]

$$\mathcal{L} = \frac{g_{eff}^2 \eta}{2\Lambda^2} \left(\bar{q} \gamma^\mu q + \mathcal{F}_\ell \bar{\ell} \gamma^\mu \ell \right)_{L/R} \left(\bar{q} \gamma_\mu q + \mathcal{F}_\ell \bar{\ell} \gamma_\mu \ell \right)_{L/R} \quad (1)$$

where the generation and color indices have been suppressed, $\eta = \pm 1$, and \mathcal{F}_ℓ is inserted to allow for different quark and lepton couplings but is anticipated to be $\mathcal{O}(1)$. Since the binding force is expected to be strong when Q^2 approaches Λ^2 , it is conventional to define $g_{eff}^2 = 4\pi$. The subscript L/R indicates that the currents in each parenthesis can be either left- or right-handed and various possible choices of the chiralities lead to different predictions for the angular distributions of the reactions where the contact terms contribute.

Interference between the contact terms and the usual gauge interactions can lead to observable deviations from SM predictions at energies lower than Λ . They can affect *e.g.*, jet production at hadron colliders, the Drell-Yan process, or lepton scattering. The size of this interference term relative to the SM amplitude is $Q^2/\alpha_i\Lambda^2$, where α_i represents the strength of the relevant gauge coupling. One may hence neglect modifications of the gauge couplings due to form factors. It is clear that the effects of the contact interactions will be most important in the phase space region with large Q^2 . At hadron colliders these terms manifest themselves in the high E_T region in jet and lepton-pair production and deviations from the SM can unfortunately often become entangled in the uncertainties associated with the parton densities[4]. CDF has recently constrained[5] $qqqq$ contact interactions from the measurement of the dijet angular distribution; it is found to be in good agreement with QCD, thereby excluding at 95 % C.L. a contact interaction among the up and down type quarks with scale $\Lambda^+ \leq 1.6$ TeV or $\Lambda^- \leq 1.4$ TeV. Composite scales of 2–5 TeV can be reached in future runs at the Tevatron[5] and a search limit for Λ in the 15–20 TeV range is expected at the LHC [6]. CDF also found the restrictions[7] $\Lambda_{LL}^- \geq 3.4$ TeV and $\Lambda_{LL}^+ \geq 2.4$ TeV at 95% C.L. on $qql\ell$ contact interactions from 110 pb $^{-1}$ of data on Drell-Yan production. Run II of the Tevatron is expected to improve these limits to ~ 10 TeV. HERA also constrains $qql\ell$ contact terms, with the exclusion[8] from H1 of $\Lambda \geq 1 - 2.5$ TeV at 95% C.L., where the range takes into account various helicity combinations. A review of the bounds on four lepton contact interactions from PEP, PETRA, TRISTAN, and ALEPH is given in Buskulic *et al.*[9], but are superseded by recent results from OPAL at $\sqrt{s} = 161$ GeV which bounds Λ in the range 1.4 – 6.6 TeV (again, for

the various helicity states) from e^+e^- , $\mu^+\mu^-$, $\tau^+\tau^-$ and combined $\ell^+\ell^-$ pair production [10]. This search also constrains $\Lambda_{eeqq} \geq 2.1 - 3.5$ TeV and $\Lambda_{eebb} \geq 1.6 - 3.7$ TeV at 95% C.L. from identified b-quark final states. There is an earlier analysis[11] of $eecc$ contact terms from the forward-backward asymmetry of D and D^* mesons which yields a bound of $\Lambda_{eecc} > 1 - 1.6$ TeV.

In this contribution, we study the compositeness search reach on $\ell\ell qq$ and $\ell\ell\ell'\ell'$ contact terms using the processes $\ell^+\ell^- \rightarrow b\bar{b}, c\bar{c}, \ell'^+\ell'^-$ where $\ell = e$ or μ at future lepton colliders. We shall consider e^+e^- colliders with center of mass energy 0.5, 1, 1.5, 5 TeV and luminosity 50, 200, 200, 1000 fb $^{-1}$, respectively, as well as muon colliders with $\sqrt{s} = 0.5, 4$ TeV and luminosity 0.7, 50, and 1000 fb $^{-1}$. We build on earlier studies[12] of compositeness searches at lepton colliders.

2 Collection of Formulae

The reactions $\ell^+\ell^- \rightarrow f\bar{f}$ where $f = \mu, \tau, b, c$ and $\ell = e, \mu$ ($\ell \neq f$) proceed via s -channel exchanges of γ and Z bosons, as well as the $\ell\ell f\bar{f}$ contact interaction. Thus, not only the squared term of the contact interaction but also the interference terms between the γ , Z exchanges and the contact interaction will contribute to the differential cross section and yield deviations from the SM. We explicitly rewrite the contact terms for $\ell\ell f\bar{f}$

$$\begin{aligned} \mathcal{L} = & \frac{4\pi}{2\Lambda^2} [\eta_{LL}(\bar{e}_L\gamma_\mu e_L)(\bar{f}_L\gamma^\mu f_L) \\ & + \eta_{LR}(\bar{e}_L\gamma_\mu e_L)(\bar{f}_R\gamma^\mu f_R) + \eta_{RL}(\bar{e}_R\gamma_\mu e_R)(\bar{f}_L\gamma^\mu f_L) \\ & + \eta_{RR}(\bar{e}_R\gamma_\mu e_R)(\bar{f}_R\gamma^\mu f_R)]. \end{aligned} \quad (2)$$

The polarized differential cross sections for $e_{L/R}^- e^+ \rightarrow f\bar{f}$ are

$$\frac{d\sigma_L}{d\cos\theta} = \frac{\pi\alpha^2 C_f}{4s} \left\{ |C_{LL}|^2 (1 + \cos\theta)^2 + |C_{LR}|^2 (1 - \cos\theta)^2 \right\} \quad (3)$$

$$\frac{d\sigma_R}{d\cos\theta} = \frac{\pi\alpha^2 C_f}{4s} \left\{ |C_{RR}|^2 (1 + \cos\theta)^2 + |C_{RL}|^2 (1 - \cos\theta)^2 \right\} \quad (4)$$

where θ is the scattering angle in the center of mass frame and C_f represents the color factor being the usual 3(1) for quarks(leptons). The helicity amplitudes are

$$\begin{aligned} C_{LL} &= -Q_f + \frac{C_L^e C_L^f}{c_w^2 s_w^2} \frac{s}{s - M_Z^2 + i\Gamma_Z M_Z} + \frac{s\eta_{LL}}{2\alpha\Lambda^2}, \\ C_{LR} &= -Q_f + \frac{C_L^e C_R^f}{c_w^2 s_w^2} \frac{s}{s - M_Z^2 + i\Gamma_Z M_Z} + \frac{s\eta_{LR}}{2\alpha\Lambda^2}, \end{aligned} \quad (5)$$

with $C_L^f = T_{3f} - Q_f s_w^2$, $C_R^f = -Q_f s_w^2$, s_w and c_w are the sine and cosine of the weak mixing angle, and Q_f and T_{3f} represent the fermion's charge and third component of the weak isospin, respectively. The expressions for C_{RR} and C_{RL} can be obtained by interchanging $L \leftrightarrow R$. The use of polarized beams, combined with the angular distributions, can thus clearly determine the helicity of the contact term.

The unpolarized differential cross section is given simply by

$$\frac{d\sigma}{d\cos\theta} = \frac{1}{2} \left[\frac{d\sigma_L}{d\cos\theta} + \frac{d\sigma_R}{d\cos\theta} \right]. \quad (6)$$

The polarized and unpolarized total cross sections are obtained by integrating over $\cos\theta$, resulting in the spin-averaged unpolarized cross section:

$$\sigma = \frac{\pi\alpha^2 C_f}{3s} \left[|C_{LL}|^2 + |C_{LR}|^2 + |C_{RL}|^2 + |C_{RR}|^2 \right]. \quad (7)$$

The forward-backward and left-right asymmetries are easily obtained and can be written as

$$A_{FB} = \frac{3}{4} \frac{|C_{LL}|^2 + |C_{RR}|^2 - |C_{LR}|^2 - |C_{RL}|^2}{|C_{LL}|^2 + |C_{RR}|^2 + |C_{LR}|^2 + |C_{RL}|^2}, \quad (8)$$

$$A_{LR} = \frac{|C_{LL}|^2 + |C_{LR}|^2 - |C_{RR}|^2 - |C_{RL}|^2}{|C_{LL}|^2 + |C_{LR}|^2 + |C_{RR}|^2 + |C_{RL}|^2}. \quad (9)$$

Figure 1 displays the $\cos\theta$ distribution for $e^+e^- \rightarrow b\bar{b}$ at $\sqrt{s} = 0.5$ TeV for the SM and with a contact term present. The effects of a contact term are qualitatively similar for other final states.

In all curves we set $|\eta| = 1$. In fig. 1a we take $\Lambda = 10$ TeV which shows that a finite value of Λ alters the angular distribution particularly in the forward direction. Fig. 1b displays the angular distributions for right-handed polarized electrons. Although the effects of contact interactions are more dramatic here, because the right-handed cross section is smaller, the relative contribution of right-handed contact terms will be smaller in unpolarized cross sections. Thus, not only will polarization be important for disentangling the helicity structure of a contact interaction should deviations be seen, but polarization will also enhance the sensitivity to contact interactions. In fig. 1c distributions are shown for $\eta_{LL} = \pm 1$ and $\eta_{RR} = \pm 1$ demonstrating that opposite signs for the η 's results in opposite interference. Finally, in fig. 1d the angular distribution is shown for η_{LL} but with $\Lambda = 5$ TeV, 10 TeV, 20 TeV, and 30 TeV to give a feeling for the sensitivity to the scale of new physics.

We note that the effects of the contact term on $e^+e^- \rightarrow q\bar{q}$ are relatively small when all quark flavors are summed, compared to the individual deviations in *e.g.*, $b\bar{b}$ or $c\bar{c}$, because cancelations occur in the interference term between the up-type and down-type quarks. We thus concentrate on the heavy quark final states, taking a 60% identification efficiency for detecting b-quarks and 35% identification efficiency for detecting c-quarks at the NLC[13]. The detection efficiency of heavy flavor final states at a muon collider has yet to be determined, but is expected to be worse than what can be achieved at the NLC due to the inability to put a vertex detector close to the interaction point and due to the heavier backgrounds. For now we assume canonical LEP values, $\epsilon_b = 25\%$, $\epsilon_c = 5\%$ for the muon collider but warn the reader that these numbers are quite arbitrary and are only used for illustrative purposes. We assume 100% identification efficiency for leptons. Although we do not take into account the purity of the tagged heavy flavor samples in our results, we note that the purities that can be achieved at a linear collider are higher than can be achieved at LEP.

3 Results

To gauge the sensitivity to the compositeness scale we assume that the SM is correct and perform a χ^2 analysis of the $\cos \theta$ angular distribution. To perform this we choose the detector acceptance to be $|\cos \theta| < 0.985$ (corresponding to $\theta = 10^\circ$) for the e^+e^- collider and $|\cos \theta| < 0.94$ (corresponding to $\theta = 20^\circ$) for the muon collider[14]. We note that angular acceptance of a typical muon collider detector is expected to be reduced due to additional shielding required to minimize the radiation backgrounds from the muon beams. We then divide the angular distribution into 10 equal bins. The χ^2 distribution is evaluated by the usual expression:

$$\chi^2 = L \times \epsilon \times \sum_{i=1}^{10} \left[\frac{\int_{\text{bin } i} \frac{d\sigma^\Lambda}{d\cos\theta} d\cos\theta - \int_{\text{bin } i} \frac{d\sigma^{SM}}{d\cos\theta} d\cos\theta}{\sqrt{\int_{\text{bin } i} \frac{d\sigma^{SM}}{d\cos\theta} d\cos\theta}} \right]^2 \quad (10)$$

where L is the luminosity and ϵ is the efficiency for detecting the final state under consideration which is discussed above. For polarized beams we assume 1/2 of the total integrated luminosity listed in the tables for each polarization. We assume that only one of the η 's is nonzero at a time.

The 95% C.L. bounds on Λ are tabulated in Tables I, II, and III[†]. Generally, high luminosity e^+e^- and $\mu^+\mu^-$ colliders are quite sensitive to contact interactions with discovery limits ranging from 5 to 50 times the center of mass energy. For unpolarized beams with leptons in the final state, the slightly higher sensitivity to contact interactions at e^+e^- colliders than at $\mu^+\mu^-$ colliders with the same \sqrt{s} can be attributed to the larger expected acceptance for e^+e^- detectors. For $b\bar{b}$ final states the sensitivities for e^+e^- colliders are roughly 20% higher than for $\mu^+\mu^-$ colliders while for $c\bar{c}$ final states the difference can be up to a factor of two. These differences are due to the different tagging efficiencies assumed for e^+e^- and $\mu^+\mu^-$ colliders. Polarization in the e^+e^- colliders can offer even higher limits depending on the final state being considered. More importantly, if deviations are observed polarization would be crucial for determining the chirality of the new interaction. Finally,

[†]The limits in this paper supersede the results presented in the New Interaction Subgroup Report by K. Cheung and R. Harris[15]

we note that for $b\bar{b}$ and $c\bar{c}$ final states sometimes very specific, relatively low values of Λ , give rise to angular distributions indistinguishable from the SM. However, we expect that these values will be ruled out by other measurements before high energy lepton colliders become operational so we only include the higher values in the tables.

4 Summary

In this report we presented the results of a preliminary study on the sensitivity to contact interactions at future high energy e^+e^- and $\mu^+\mu^-$ colliders. Depending on the specific collider and final state, contact interactions can be detected up to 5-50 times the center of mass energy of the collider with the lowest number coming from the low luminosity 500 GeV $\mu^+\mu^-$ collider and the highest numbers from high luminosity e^+e^- colliders with polarization. These results should be taken as preliminary. First and foremost the sensitivities were based only on statistical errors and systematic errors were not included. In addition, a more thorough analysis should include potentially important effects like initial state radiation and should consider heavy quark final state purities. These considerations are under study and will be presented elsewhere [16].

Acknowledgements

S.G. thanks Dean Karlen for helpful conversations.

References

- [1] See, for example, H. Harari, Phys. Rept. **104**, 159 (1984); W. Buchmüller, Acta Phys. Austriaca Suppl. XXVII, 517 (1985); W. Buchmüller and D. Wyler, Nucl. Phys. **B268**, 621 (1986).
- [2] E. Eichten *et al.*, Phys. Rev. Lett. **50**, 811 (1983).
- [3] E. Eichten and K. Lane, in these proceedings.

Table 1: 95% C.L. compositeness search reach in TeV for e^+e^- colliders.

process	Λ_{LL}	Λ_{LR}	Λ_{RL}	Λ_{RR}
$\sqrt{s} = 0.5 \text{ TeV}, L=50 \text{ fb}^{-1}$				
$e_L^- e^+ \rightarrow \mu^+ \mu^-$ (P=1.0)	33	30	—	—
$e_L^- e^+ \rightarrow \mu^+ \mu^-$ (P=0.9)	32	29	10	10
$e_R^- e^+ \rightarrow \mu^+ \mu^-$ (P=1.0)	—	—	30	33
$e_R^- e^+ \rightarrow \mu^+ \mu^-$ (P=0.9)	11	10	29	31
$e^- e^+ \rightarrow \mu^+ \mu^-$	28	26	26	27
$e_L^- e^+ \rightarrow b\bar{b}$ (P=1.0)	39	32	—	—
$e_L^- e^+ \rightarrow b\bar{b}$ (P=0.9)	38	30	5.3	9.1
$e_R^- e^+ \rightarrow b\bar{b}$ (P=1.0)	—	—	35	38
$e_R^- e^+ \rightarrow b\bar{b}$ (P=0.9)	17	12	33	33
$e^- e^+ \rightarrow b\bar{b}$	37	28	28	25
$e_L^- e^+ \rightarrow c\bar{c}$ (P=1.0)	34	29	—	—
$e_L^- e^+ \rightarrow c\bar{c}$ (P=0.9)	33	28	5.0	8.5
$e_R^- e^+ \rightarrow c\bar{c}$ (P=1.0)	—	—	27	34
$e_R^- e^+ \rightarrow c\bar{c}$ (P=0.9)	12	11	24	32
$e^- e^+ \rightarrow c\bar{c}$	31	28	18	26
$\sqrt{s} = 1 \text{ TeV}, L=200 \text{ fb}^{-1}$				
$e_L^- e^+ \rightarrow \mu^+ \mu^-$ (P=1.0)	66	60	—	—
$e_L^- e^+ \rightarrow \mu^+ \mu^-$ (P=0.9)	63	57	20	21
$e_R^- e^+ \rightarrow \mu^+ \mu^-$ (P=1.0)	—	—	61	66
$e_R^- e^+ \rightarrow \mu^+ \mu^-$ (P=0.9)	22	20	58	62
$e^- e^+ \rightarrow \mu^+ \mu^-$	57	51	51	55
$e_L^- e^+ \rightarrow b\bar{b}$ (P=1.0)	78	64	—	—
$e_L^- e^+ \rightarrow b\bar{b}$ (P=0.9)	75	61	11	18
$e_R^- e^+ \rightarrow b\bar{b}$ (P=1.0)	—	—	70	76
$e_R^- e^+ \rightarrow b\bar{b}$ (P=0.9)	34	24	65	67
$e^- e^+ \rightarrow b\bar{b}$	74	56	55	50
$e_L^- e^+ \rightarrow c\bar{c}$ (P=1.0)	68	59	—	—
$e_L^- e^+ \rightarrow c\bar{c}$ (P=0.9)	65	57	9.9	17
$e_R^- e^+ \rightarrow c\bar{c}$ (P=1.0)	—	—	55	68
$e_R^- e^+ \rightarrow c\bar{c}$ (P=0.9)	24	22	49	62
$e^- e^+ \rightarrow c\bar{c}$	61	55	37	51

Table 2: 95% C.L. compositeness search reach in TeV for e^+e^- colliders.

process	Λ_{LL}	Λ_{LR}	Λ_{RL}	Λ_{RR}
$\sqrt{s} = 1.5 \text{ TeV}, L=200 \text{ fb}^{-1}$				
$e_L^- e^+ \rightarrow \mu^+ \mu^-$ (P=1.0)	81	74	—	—
$e_L^- e^+ \rightarrow \mu^+ \mu^-$ (P=0.9)	77	70	25	26
$e_R^- e^+ \rightarrow \mu^+ \mu^-$ (P=1.0)	—	—	74	81
$e_R^- e^+ \rightarrow \mu^+ \mu^-$ (P=0.9)	27	25	70	76
$e^- e^+ \rightarrow \mu^+ \mu^-$	70	63	63	67
$e_L^- e^+ \rightarrow b\bar{b}$ (P=1.0)	95	80	—	—
$e_L^- e^+ \rightarrow b\bar{b}$ (P=0.9)	92	77	15	23
$e_R^- e^+ \rightarrow b\bar{b}$ (P=1.0)	—	—	84	94
$e_R^- e^+ \rightarrow b\bar{b}$ (P=0.9)	41	31	78	82
$e^- e^+ \rightarrow b\bar{b}$	90	70	66	61
$e_L^- e^+ \rightarrow c\bar{c}$ (P=1.0)	83	72	—	—
$e_L^- e^+ \rightarrow c\bar{c}$ (P=0.9)	80	69	14	20
$e_R^- e^+ \rightarrow c\bar{c}$ (P=1.0)	—	—	67	83
$e_R^- e^+ \rightarrow c\bar{c}$ (P=0.9)	29	26	60	76
$e^- e^+ \rightarrow c\bar{c}$	75	67	44	63
$\sqrt{s} = 5 \text{ TeV}, L=1000 \text{ fb}^{-1}$				
$e_L^- e^+ \rightarrow \mu^+ \mu^-$ (P=1.0)	220	200	—	—
$e_L^- e^+ \rightarrow \mu^+ \mu^-$ (P=0.9)	210	190	70	71
$e_R^- e^+ \rightarrow \mu^+ \mu^-$ (P=1.0)	—	—	200	220
$e_R^- e^+ \rightarrow \mu^+ \mu^-$ (P=0.9)	75	70	190	210
$e^- e^+ \rightarrow \mu^+ \mu^-$	190	170	170	180
$e_L^- e^+ \rightarrow b\bar{b}$ (P=1.0)	260	220	—	—
$e_L^- e^+ \rightarrow b\bar{b}$ (P=0.9)	250	210	49	66
$e_R^- e^+ \rightarrow b\bar{b}$ (P=1.0)	—	—	230	250
$e_R^- e^+ \rightarrow b\bar{b}$ (P=0.9)	110	89	210	220
$e^- e^+ \rightarrow b\bar{b}$	250	200	180	170
$e_L^- e^+ \rightarrow c\bar{c}$ (P=1.0)	220	190	—	—
$e_L^- e^+ \rightarrow c\bar{c}$ (P=0.9)	210	190	43	46
$e_R^- e^+ \rightarrow c\bar{c}$ (P=1.0)	—	—	180	220
$e_R^- e^+ \rightarrow c\bar{c}$ (P=0.9)	78	38	160	210
$e^- e^+ \rightarrow c\bar{c}$	200	180	110	170

Table 3: 95% C.L. compositeness search reach in TeV for $\mu^+\mu^-$ colliders.

process	Λ_{LL}	Λ_{LR}	Λ_{RL}	Λ_{RR}
$\sqrt{s} = 0.5 \text{ TeV}, L=0.7 \text{ fb}^{-1}$				
$\mu^+\mu^- \rightarrow \tau^+\tau^-$	9.8	9.1	9.1	9.4
$\mu^+\mu^- \rightarrow b\bar{b}$	10	8.8	4.9	7.6
$\mu^+\mu^- \rightarrow c\bar{c}$	5.6	3.6	4.2	2.7
$\sqrt{s} = 0.5 \text{ TeV}, L=50 \text{ fb}^{-1}$				
$\mu^+\mu^- \rightarrow \tau^+\tau^-$	28	25	25	27
$\mu^+\mu^- \rightarrow b\bar{b}$	29	22	21	20
$\mu^+\mu^- \rightarrow c\bar{c}$	19	16	5.7	15
$\sqrt{s} = 4 \text{ TeV}, L=1000 \text{ fb}^{-1}$				
$\mu^+\mu^- \rightarrow \tau^+\tau^-$	170	150	150	160
$\mu^+\mu^- \rightarrow b\bar{b}$	180	140	120	120
$\mu^+\mu^- \rightarrow c\bar{c}$	110	92	42	90

- [4] CDF Collaboration (F. Abe *et al.*), Phys. Rev. Lett. **77**, 438 (1996); R. Brock, plenary talk at the *28th International Conference on High Energy Physics*, Warsaw, Poland, July 1996.
- [5] CDF Collaboration (F. Abe *et al.*), Fermilab-Pub-96/317-E.
- [6] U.S. ATLAS and U.S. CMS Collaborations, edited by I. Hinchliffe and J. Womersley, LBNL-38997 (1996).
- [7] P. de Barbaro *et al.*, these proceedings.
- [8] H1 Collaboration (S. Aid *et al.*), Phys. Lett. **B353**, 578 (1995).
- [9] ALEPH Collaboration (D. Buskulic *et al.*), Z. Phys. **C59**, 215 (1993).
- [10] OPAL Collaboration (K. Ackerstaff *et al.*), CERN Report CERN-PPE/96-156 (1996).
- [11] K. Hagiwara *et al.*, Phys. Lett. **B219**, 369 (1989).
- [12] B. Schrempp *et al.*, Nucl. Phys. **B296**,1 (1988); E.N. Argyres *et al.*, Nucl. Phys. **B354**, 1 (1991); J. Ellis, and F. Pauss, *Proceedings of the Workshop on Physics at Future Accelerators*, La Thuile, Italy, CERN 87-07 (1987).
- [13] C. Damerall, and D. Jackson, these proceedings.
- [14] NLC Accelerator Design Group and Physics Working Group, (S. Kulhman *et al.*), *Physics and Technology of the Next Linear Collider*, BNL-52502 (1996); $\mu^+\mu^-$ Collider Collaboration (R. Palmer *et al.*), $\mu^+\mu^-$ Collider: A Feasibility Study, BNL-52503 (1996).
- [15] K. Cheung and R. Harris, these proceedings.
- [16] K. Cheung, S. Godfrey, and J. Hewett, in progress.

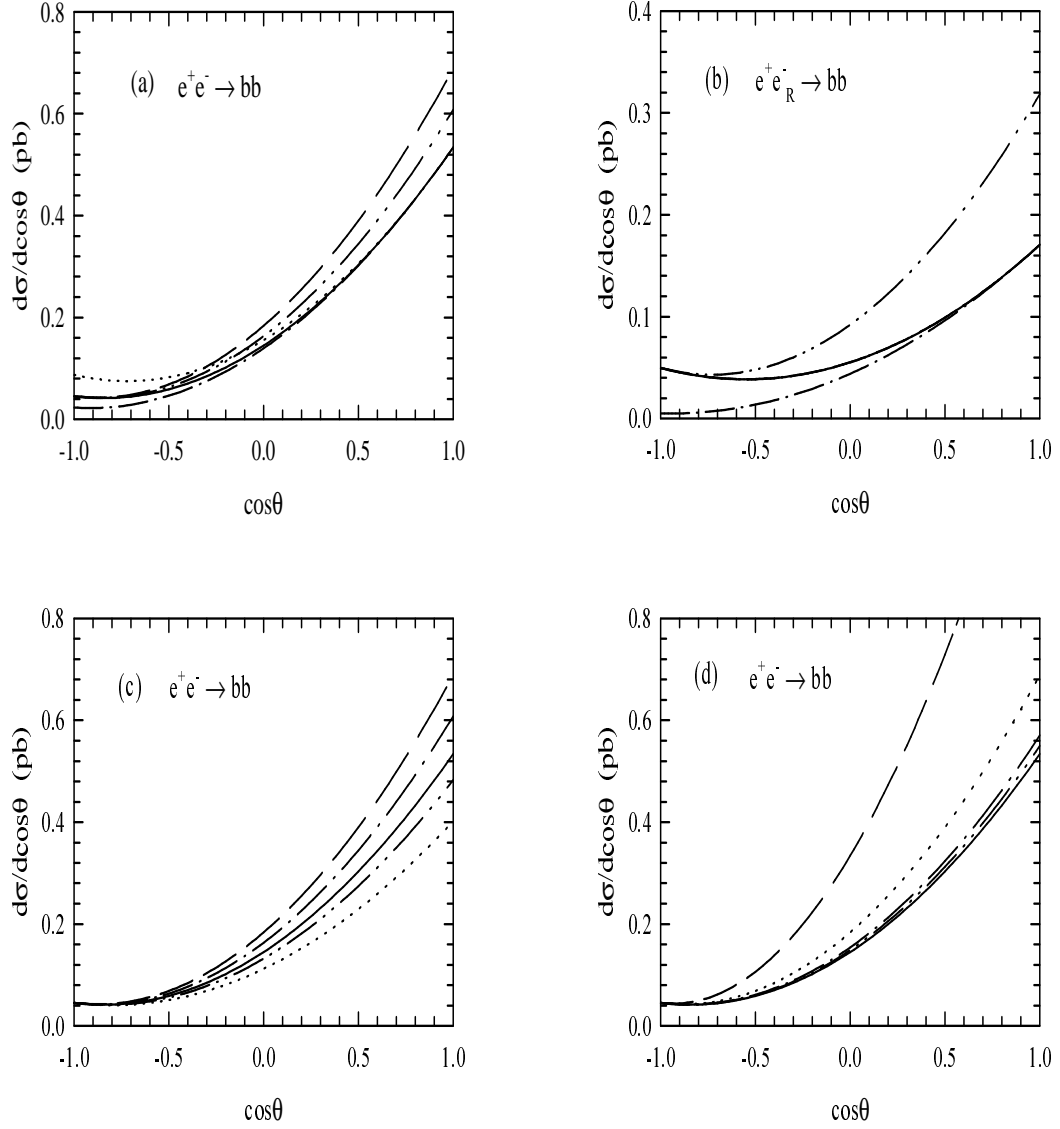


Figure 1: The $\cos\theta$ distribution for $e^+e^- \rightarrow b\bar{b}$ at $E_{CM} = 0.5$ TeV with $\Lambda = 10$ TeV everywhere except for (d). In all cases the solid line is for the SM ($\Lambda = \infty$). (a) Unpolarized e^+e^- with $\eta_{LL} = +1$ (dashed), $\eta_{LR} = +1$ (dotted), $\eta_{RL} = +1$ (dot-dashed), and $\eta_{RR} = +1$ (dot-dot-dashed). (b) Polarized e^+e^- with $\eta_{RL} = +1$ (dot-dashed) and $\eta_{RR} = +1$ (dot-dot-dashed). (c) Unpolarized e^+e^- with $\eta_{LL} = +1, -1$ (dashed, dotted), $\eta_{RR} = +1, -1$ (dot-dashed, dot-dot-dashed). (d) Unpolarized e^+e^- with $\eta_{LL} = +1$ with $\Lambda = 5, 10, 20, 30$ TeV (dashed, dotted, dot-dashed, dot-dot-dashed).